

Article

Migration and Transformation of Vanadium and Nickel in High Sulfur Petroleum Coke during Gasification Processes

Wei Li ¹, Ben Wang ^{1,*}, Jun Nie ¹, Wu Yang ¹, Linlin Xu ² and Lushi Sun ^{1,*}

¹ State Key Laboratory of Coal Combustion, Huazhong University of Science and Technology, Wuhan 430074, China; liwei2017@hust.edu.cn (W.L.); u201011707@hust.edu.cn (J.N.); m201671234@hust.edu.cn (W.Y.)

² Wuhan Huayu Energy-Burning Engineering Technology Co. Ltd., G3, New Energy Building, Future City, No. 999 Gaoxin Avenue, East Lake High-tech Zone, Wuhan 430206, China; xulinlin@huayuceet.com

* Correspondence: benwang@hust.edu.cn (B.W.); sunlushi@hust.edu.cn (L.S.); Tel.: +86-27-87542417 (B.W.); +86-27-87542417 (L.S.)

Received: 26 July 2018; Accepted: 14 August 2018; Published: 18 August 2018



Abstract: The volatilization characteristics and occurrence forms of V and Ni in petroleum coke (petcoke) were investigated during steam (H₂O) and carbon dioxide (CO₂) gasification on a fixed bed reactor at 800–1100 °C. The Tessier sequential chemical extraction procedure was employed to determine the different forms of V and Ni. The results showed their volatilities were not dependent on the gasification atmosphere, but rather relied mainly on the reaction temperature. The CO₂ atmosphere accelerated the conversion of organic-bound nickel to residual form at low temperature and promoted Fe-Mn oxides formation at high temperature. However, the H₂O atmosphere was conducive to form vanadium bound to Fe-Mn oxides and promoted the decomposition of residual forms. In addition, the thermodynamic equilibrium calculations showed the volatilization of Ni mainly released Ni₃S₂ between 800–1100 °C. The H₂O atmosphere was favorable to generate the more stable Ni_xS_y compound, thereby suppressing the volatilization of Ni, while the presence of CO₂ led to an increase in residual V and decrease of Fe-Mn oxides. The V and Ni mainly caused erosion problems under the CO₂ atmosphere while the fouling and slagging obviously increased under the H₂O atmosphere with impacts gradually weakened with the increase of temperature.

Keywords: high sulfur petcoke; vanadium; nickel; gasification; sequential extraction; migration

1. Introduction

The shortage of energy resources and the improvement of petroleum processing capacity have led to a continuous increase in the production of petcoke [1–3]. Petcoke is mainly used in the electrolytic aluminum industry and boilers as a combustion fuel, however it releases massive amounts of polluting gases such as SO₂ under combustion conditions, resulting in serious environmental problems [4]. Petcoke has high calorific value, low ash and low price qualities, which endow petcoke with the potential to be a gasification feedstock to produce synthetic gas and recycle sulfur through the Claus process. Therefore, it is an efficient and clean utilization way, which has broad prospects for making waste profitable [5,6]. Unfortunately, petcoke is enriched with Ni and V concentrations of more than 1000 ppm, resulting in serious fouling, slagging and erosion problems of gasification equipment and pipes [7]. V₂O₅ can react with refractory and metal oxides [8], exposing the surface of the metal to an oxidizing atmosphere and accelerating its oxidation rate. High concentrations of V, Ni and sulfur in petcoke can cause severe pollution, including erosion and corrosion to the furnace and equipment, during gasification [9]. Therefore, a thorough understanding of the chemical speciation migration of V and Ni in the process of gasification and the complex chemical reactions that may occur with

gas reactants and mineral components is important to predict and control the fouling, slagging and erosion behavior during the process of gasification.

There are three gasification technologies, including fixed bed, fluidized bed, and entrained flow bed, of which the entrained flow bed appears to be a promising gasification technology with the advantages of high output, high thermal conversion efficiency because of its higher operating temperatures. However, the high temperature also accelerates the fouling, slagging and erosion problems caused by vanadium and nickel in the petcoke. Park et al. [10] investigated slagging of petroleum coke ash. The main components of petcoke under gasification conditions were vanadium, nickel and iron. Among them, vanadium existed in the form of V_2O_3 with a melting point of up to 1940 °C. V_2O_3 in petcoke ash remained solid at the typical gasification temperature and the solid V_2O_3 caused the slag viscosity to increase. For the petcoke with high ash content, the effect of V_2O_3 on slag viscosity must be taken into consideration when the minimum gasification temperature was estimated. Nakano et al. [11] studied a synthetic slag and found that V_2O_3 could form solid solutions with Al_2O_3 and Fe_2O_3 to reduce the slag viscosity. Duchesne et al. [12] examined the viscosity characteristics of coal and petcoke blended ash. Petcoke ash was mainly composed of V and Ni, and the spinel formed by vanadium could increase the ash viscosity. Mahapatra et al. [13] measured the release of vanadium and nickel during the pyrolysis process, reporting that vanadium and nickel tended to accumulate in the coke compared to fly ash. Wang et al. [7] investigated that the formation of ash and slag was closely related to the conversion of vanadium, nickel, and sulfur during the gasification process. Brüggemann et al. [14] also observed that large amounts of gaseous nickel-containing compounds were formed in the synthesis gas. Therefore, the above problems can be relieved by using a relatively low reaction temperature.

The investigation of the occurrence and migration behavior of V and Ni has been studied by many researchers. Querol et al. and Dai, et al. [15,16] expressed that vanadium existed in the form of organic matter and aluminosilicate minerals in coal. Brüggemann et al. [14] indicated that nickel was transformed into Ni_xS_y and elemental Ni under high H_2S and low H_2S partial pressure, which was calculated from the thermodynamics of the conversion of Ni during heavy oil gasification. Wang et al. [17] found that V_2O_5 reacts with CaO to form $Ca_3V_2O_8$ when blended with coal ash in a reducing atmosphere, and the decomposition of $Ca_3V_2O_8$ could react with Fe_2O_3 to form FeV_2O_4 when the temperature was over 1300 °C. Li et al. [18] reported that the vanadium reacted with the mineral component to form a new thermal stable compound when the gasification temperature was above 1300 °C. However, a detailed systematic research on primary speciation of V and Ni in petcoke and its release and migration characteristics during gasification has not been accomplished.

Therefore, in this study, the behavior of V and Ni in the CO_2 and H_2O gasification of petcoke was studied by fixed bed gasification experiments. The Tessier sequential chemical extraction procedure and ICP-MS were used to obtain the forms of V and Ni in the gasification product under different gasification conditions. Furthermore, the release and transformation mechanism of V and Ni were elaborated deeply. Moreover, thermodynamic equilibrium calculations, the use of the FACTSAGE software, were carried out to study the reaction mechanism of V and Ni with the main associated mineral elements during gasification. Finally, a detailed assessment on the pernicious effects on gasification equipment by the mineral elements V and Ni was gained.

2. Experiments

2.1. Petcoke Samples

The petcoke samples were obtained from the Wuhan branch of Sinopec, ground and sieved through 100 mesh sieves. Before the gasification experiment, the samples were dried at 80 °C in advance in a vacuum drying oven for 24 h. The petcoke ash was prepared at 805 °C for 2 h according to the Chinese standard procedures (GB/T 1574-2007). Table 1 shows the ultimate and proximate analysis of the samples. Table 2 lists the ash compositions (by XRF) of the petcoke.

Table 1. Proximate and ultimate analysis of petcoke samples (wt %).

M_{ad}	A_{ad}	V_{ad}	FC_{ad}	C_{ad}	H_{ad}	N_{ad}	S_{ad}	O_{ad}^*
1.46	0.50	8.56	89.48	85.43	3.63	1.81	2.01	7.12

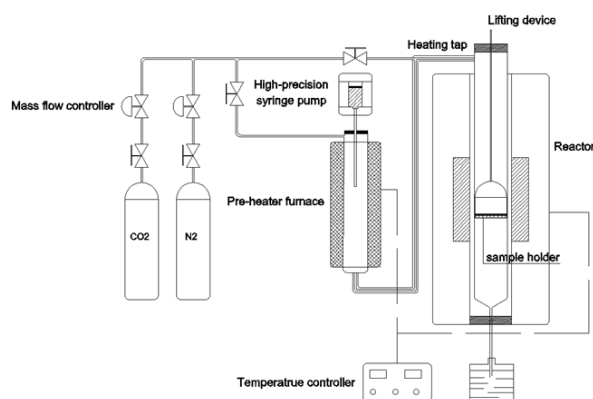
$_{ad}$: the proximate and ultimate analysis of the samples are on the air-dry basis; *: the ultimate analysis of O is quantified by the subtraction method.

Table 2. Ash composition of petcoke samples (wt %).

NiO	V_2O_5	Fe_2O_3	SiO_2	SO_3	Al_2O_3	TiO_2	CaO	Na_2O	MnO
20.11	14.88	9.41	18.18	3.87	13.59	0.96	14.54	4.29	0.17

2.2. Fixed Bed Gasification Apparatus and Experimental Procedures

Our laboratory-scale reactor system (Figure 1) contains a steam generator and a fixed-bed reactor that is heated by an electrical furnace. The total length of the quartz tube is 500 mm and the inner diameter is 40 mm. The quartz tube is heated by an electrothermal furnace, which can reach a maximum temperature of 1100 °C under control by a temperature controller. The steam generator is mainly composed of an electrical heating furnace and a high-precision syringe pump which precisely controls the water injection (0.736 mL/min of deionized water provides 1.00 L/min steam at ambient temperature). The deionized water is evaporated in the preheating furnace, and then carried by the carrier gas of N_2 . The mixture gas enters the quartz tube through a heat insulating pipeline wrapped with a heating tape.

**Figure 1.** Diagram of the fixed bed gasification system.

In the petcoke gasification experiments, a N_2 flow of 500 mL/min was maintained to remove air from the system. When the specified temperature was reached, the atmosphere was switched to carbon dioxide gas or steam carried by nitrogen. The flow rate of CO_2 was kept at 500 mL/min for all CO_2 gasification experiments, while that of N_2 was kept at 150 mL/min and H_2O at 350 mL/min for all H_2O gasification experiments, respectively. Meanwhile, basket with 1 g samples was rapidly placed in the quartz mesh in the reaction zone. The reaction time was 30 min. After gasification, the basket was pulled to the up and cold position and rapidly cooled to room temperature by N_2 . The gasification chars were collected, weighted, and subsequently analyzed.

2.3. Sequential Chemical Extraction

Sequential chemical extraction was an effective way to quantify the chemical forms of trace elements [19–21]. In this research, five chemical forms of V and Ni in petcoke and char after gasification were extracted by the Tessier sequential extraction procedure [22]. In the extraction procedures [23],

the Ni and V were extracted and partitioned into five forms: (1) exchangeable, extracted by MgCl_2 (1 mol/L); (2) bound to carbonates, extracted by CH_3COONa (1 mol/L); (3) bound to Fe-Mn oxides, extracted by $\text{NH}_2\text{OH}\cdot\text{HCl}$ (0.04 mol/L) which dissolved in CH_3COOH (25%, v/v); (4) bound to organic matter, extracted by HNO_3 (0.02 mol/L) and H_2O_2 (30%, v/v); After four extraction steps, Ni and V still remaining in the residue were labeled as residual forms, which might be present in the insoluble organic matrix or occur in minerals such as aluminosilicates, titanium dioxide, zircon, sulphides and so on [18,24].

2.4. Calculation of V and Ni Volatility

The V and Ni contents in petcoke and its gasification char and their extracted solutions were measured by inductively coupled plasma mass spectrometry (ICP-MS). V and Ni volatility is determined by the equation:

$$Rv(\%) = \left(1 - \frac{C_1 m_1}{C_0 m_0}\right) \times 100\% = \left(1 - \frac{C_1 R_y}{C_0}\right) \times 100\% \quad (1)$$

Char yield after petcoke gasification is calculated by R_y , which is assessed as follows:

$$R_y(\%) = \left(\frac{m_1}{m_0}\right) \times 100\% \quad (2)$$

where Rv is the volatility of V or Ni, %; R_y is the yield of gasification char, %; C_1 , the concentration of the V or Ni in gasification char, ug/g; C_0 , the concentration of V or Ni in petcoke, ug/g; m_1 , the weight of gasification char, g; m_0 , the weight of petcoke, g.

2.5. Thermodynamic Equilibrium Calculations

The FACTSAGE program is used to facilitate our explanation of the transformation mechanisms of V and Ni during gasification and verify the experimental results. FACTSAGE [25] software is based on the Gibbs energy minimization method. The Equilib module utilized with the FactPS and FToxid databases can detect the concentration of chemical species when specific elements or compounds react to equilibrium. The precision of the software can meet the demands of simulation. In this research, modeling employed main trace elements on behalf of the main composition of petcoke. Simulation calculations were carried under the temperature range between 100 °C to 1500 °C at normal atmospheric pressure. The quantity of petcoke feedstock to be fed to the gasifier was 1 kg and the CO_2 or H_2O was 1.5 kg. It was noticeable that the quantity of gasification agent and mineral elements was in units of g/kg-petcoke in the gasification experiment. However, the unit (g/kg-petcoke) was modified to mol/kg-petcoke for the purpose of calculation. The input information is listed in Table 3. There is an assumption that all the sulfur in petcoke is presented in the vapor phase as H_2S (g) initially because all of gasifiers produce H_2S (g) [18,26].

Table 3. Input information into the FACTSAGE.

Reactants	mol/kg-Raw Petcoke	Reactants	mol/kg-Raw Petcoke
CO	71.19	NiO	1.31×10^{-2}
H ₂	17.52	V ₂ O ₅	0.40×10^{-2}
N ₂	0.65	Fe ₂ O ₃	0.29×10^{-2}
H ₂ S	0.63	SiO ₂	1.49×10^{-2}
CO ₂ *1	34.00	Al ₂ O ₃	0.65×10^{-2}
H ₂ O *2	83.33	TiO ₂	0.06×10^{-2}
-	-	CaO	1.27×10^{-2}
-	-	Na ₂ O	0.34×10^{-2}
-	-	MnO	0.01×10^{-2}

*1 only in the CO_2 gasification, *2 only in the H_2O gasification.

3. Results and Discussion

3.1. The Char Yield from Two Types of Gasification Atmospheres

The char yield under CO₂ and H₂O gasification conditions are shown in Figure 2. The yield tends to decrease with increasing gasification temperatures. The char reduces from 89.8% (800 °C) to 64.9% (1100 °C) in CO₂ gasification while the char yield declines from 80.8% (800 °C) to 29.0% (1100 °C) in H₂O gasification. Apparently, the atmosphere plays an important role for the yield of char and petcoke has high gasification reactivity under H₂O atmosphere. From the reduction trend of char yield, it can be seen there are two stages in the CO₂ and H₂O gasification. In stage 1 (before 1000 °C), the reduction trend of char yield in H₂O atmosphere is dramatically higher than that in CO₂ atmosphere. It is interesting that the reduction trend of char yield in the CO₂ and H₂O gasification in stage 2 (after 1000 °C) is opposite to stage 1 because CO₂ molecules can cross the reaction energy barrier leading to an increase of the char consumption yield while the H₂O gasification almost complete at this temperature.

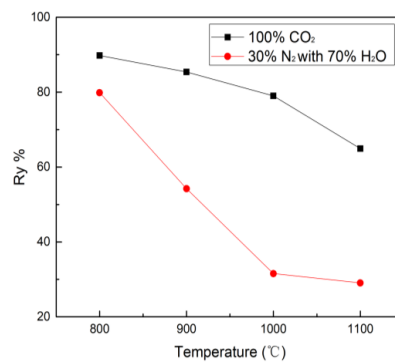


Figure 2. Char yield (Ry%) during petcoke gasification from 800 °C to 1100 °C.

3.2. Occurrence Modes of Nickel in Petcoke and Its Gasification Char

The migration of occurrence forms of nickel during CO₂ and H₂O gasification is shown in Figure 3a,b. A few Fe-Mn oxides with a proportion of 7.9% is in the raw petcoke while the content of nickel exists in exchangeable and carbonates are tiny amounts of 0.7% and 0.3%. The majority of nickel is in organic (62.7%) and residual form (28.4%). After gasification, significant change of the different forms of nickel occurs in the gasification char.

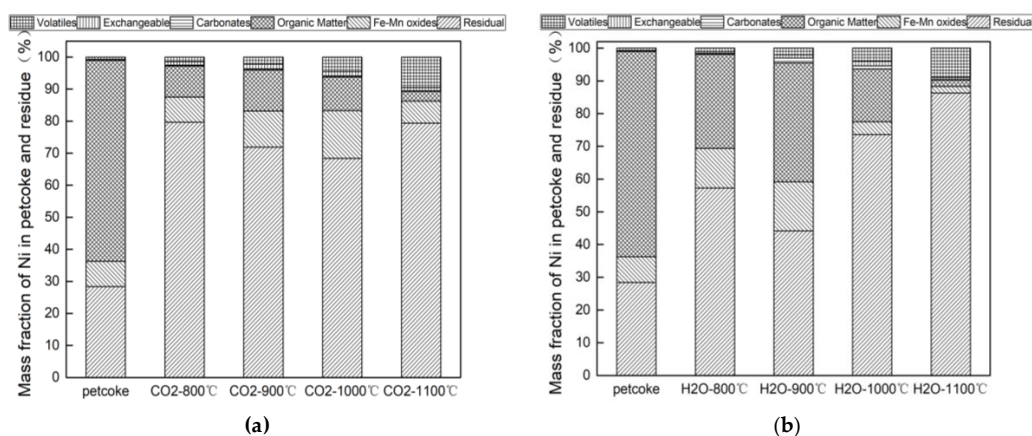


Figure 3. (a) Occurrence modes of Ni in raw petcoke and char in CO₂ atmosphere; (b) Occurrence modes of Ni in raw petcoke and char in H₂O atmosphere.

For the CO₂ gasification, as shown in Figure 3a, when the gasification temperature increases to 800 °C, most of the organic-bound nickel is converted to the residual form. The residual form of nickel increases from 28.4% to 79.7% while the content of organic-bound sharply reduces from 62.7% to 9.7%. The Ni bound to Fe-Mn oxides is basically constant. As the gasification temperature increases from 800 °C to 900 °C, the residual form of nickel begins to decompose and mainly transforms into organic and Fe-Mn oxides. At 1000 °C, the fraction of the organic-bound nickel also transforms into Fe-Mn oxides which reaches a maximum of 14.9%. When the temperature reaches 1100 °C, organic and Fe-Mn oxides are significantly reduced and converted into the residual form of nickel. The content of the residual form of nickel reaches 79.4%, which is basically consistent with the content in the residue of nickel form at 800 °C. We note that comparing the char samples at 800 °C and 1100 °C, it can be found that the content of nickel affiliated with the exchangeable, carbonates, Fe-Mn oxides and residual forms are basically unchanged. After gasification at 800 °C, Ni associated with organic matter sharply drops 53.0% while the residual form rises acutely (51.3%) and very low level of volatile Ni (1.4%) emerges. At 1100 °C, as residual form remains unchanged, Ni affiliated with organic matter further decreases 6.7% and converts into volatile Ni. In this sense, from room temperature to 1100 °C, there are 51.3% and 6.7% of organic matter Ni converted into residual form and volatile form, respectively. It can be deduced that the organic-bound nickel prefers to form residual fraction rather than volatilize.

For the H₂O gasification, as shown in Figure 3b, a large amount of organic-bound nickel decomposes from 62.7% to 28.7% and is mainly converted into the residual form (from 28.7% to 57.3%), with a small part converted into Fe-Mn oxides at 800 °C. The residual form of nickel decreases by 13.1% at 900 °C and is mainly converted into organic and Fe-Mn oxides, while the transformation behavior from 900 °C to 1000 °C shows an opposite trend. When the temperature reaches 1100 °C, organic and Fe-Mn oxides completely decompose and convert into the residual form.

In general, the gasification temperature mainly affects the transformation of the organic-bound nickel and the residual form nickel, accompanied by a small amount of other forms. Comparing the CO₂ and H₂O gasification processes, the trends of the different forms are roughly the same, but the contents differs greatly. At 800–900 °C, the new generated residual form nickel in CO₂ atmosphere is nearly three times higher than that of H₂O atmosphere, indicating that CO₂ atmosphere is conducive to the conversion of the organic-bound nickel to the residual form at low temperature. At 1000–1100 °C, the organic-bound and the residual form nickel in the CO₂ atmosphere are lower than in the H₂O atmosphere, indicating that the CO₂ atmosphere promotes the formation of Fe-Mn oxides at high temperature. In both atmospheres, the organic-bound nickel gradually decreases with temperature, but the amount in the H₂O one is significantly higher than that in the CO₂ atmosphere, indicating that the CO₂ gasification are favorable to the decomposition of organic-bound nickel. The trends of the residual form Fe-Mn oxides are also generally the same. The main difference is that the peak of the content of Fe-Mn oxides in H₂O atmosphere is advanced to 900 °C, which is probably due to the relatively low activity of CO₂ and the decomposition of bound to Fe-Mn oxides requires higher energy to carry out, leading to the transformation of most of Fe-Mn oxides into the residual form of nickel at 1000 °C under CO₂ atmosphere.

As the temperature increases, the volatilization characteristic of nickel gradually increases during H₂O and CO₂ gasification, illustrated in Figure 4. It is remarkable that H₂O and CO₂ gasification display similar volatilization behavior. The nickel volatility in H₂O and CO₂ gasification reaches the highest *R_v* value 9.0% and 9.5% at 1100 °C. It is apparent that the difference in the nickel volatility between H₂O and CO₂ gasification is ignorable, so it can be concluded that the volatility of nickel is not dependent on the gasification atmosphere, but rather mainly on the reaction temperature.

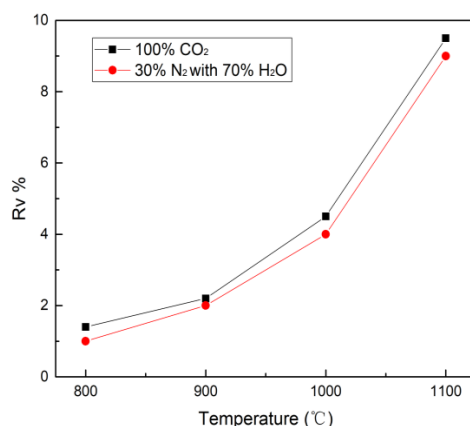


Figure 4. Volatility ($Rv\%$) of nickel during petcoke gasification from 800 °C to 1100 °C.

3.3. Occurrence Modes of Vanadium in Petcoke and Its Gasification Char

The transformation of different forms of vanadium in the process of CO₂ and H₂O gasification can be seen from Figure 5a,b. The mass fraction of vanadium bound to exchangeable and carbonates can be barely detected by ICP-AES. The occurrence of vanadium in petcoke, which is similar to that of nickel, is mainly in organic matter (65.78%) and residual form (28.29%), with a small amount of Fe-Mn oxides form, which is consistent with Li et al. [18] who reached the conclusion that the organic and residual forms are the predominant vanadium chemical forms while the content of vanadium occurring in exchangeable, carbonates, and Fe-Mn oxides are negligible for raw petcoke.

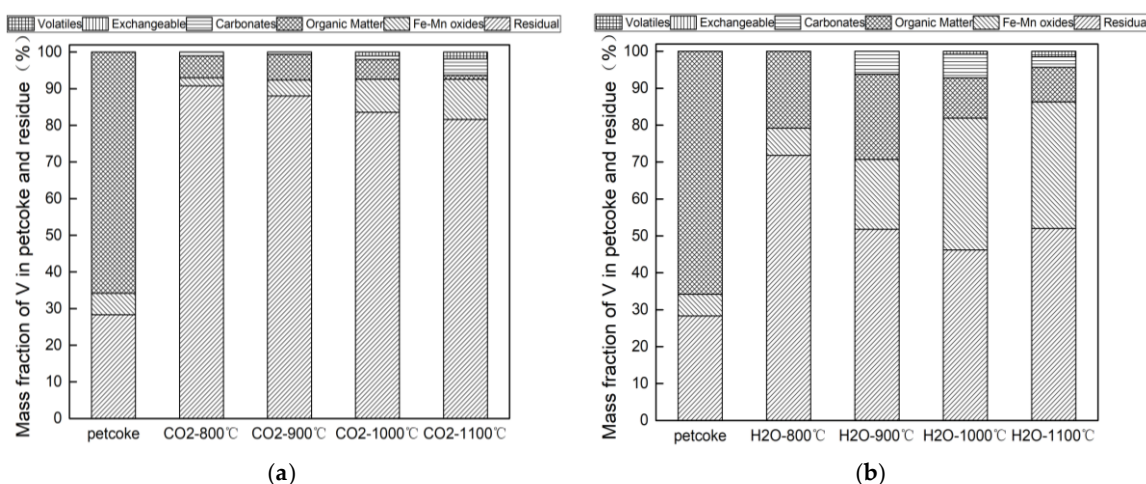


Figure 5. (a) Occurrence modes of V in raw petcoke and char in CO₂ gasification; (b) Occurrence modes of V in raw petcoke and char in H₂O gasification.

For the CO₂ gasification, most of the organic-bound vanadium converts to the residual form of vanadium at 800 °C. The content of the organic-bound vanadium sharply reduces from 65.8% to 6.0% and the vanadium bound to Fe-Mn oxides decreases from 5.9% to 2.2%, resulting in the residual form vanadium reaching a maximum of 90.8%. As temperature increases to 1000 °C, the residual form of vanadium begins to decompose, mainly converting into vanadium bound to Fe-Mn oxides, while the other forms remain basically unchanged. When the temperature reaches 1100 °C, the Fe-Mn oxides reach the maximum value of 11.0%, while the organic-bound vanadium is almost completely decomposed. After gasification at 800 °C, V associated with organic matter sharply drops 59.8%, while the residual form acutely rises 62.5% with no content of V volatility emerging. At 1100 °C,

V associated with organic matter decreases 64.7% while the residual form acutely rises 53.3% with a little V volatility (1.8%) emerging. It is obvious that the organic-bound vanadium prefers to form residual fraction rather than volatilize. No vanadium bound to exchangeable is found throughout the whole gasification process.

For the H₂O gasification, as shown in Figure 5b the organic-bound vanadium decomposes to the residual form at 800 °C. The organic-bound vanadium sharply reduces from 65.8% to 20.8% and the residual form increases from 28.3% to 71.8%. At 900 °C, the residual form of vanadium decreases by 20.0% and changes to the Fe-Mn oxides and carbonates while the organic-bound vanadium remains consistent. As the temperature increases to 1000 °C, both organic-bound and the residual form of vanadium simultaneously reduce and convert into Fe-Mn oxides while the carbonates remains constant. At 1100 °C, the vanadium bound to carbonates converts to the residual form. The organic-bound vanadium shows a downward trend while Fe-Mn oxides display an upward tendency during steam gasification. No vanadium bound to exchangeable is detected.

Comparing the two kinds of atmosphere, the variation of the forms are obviously different. In the CO₂ atmosphere, the dominant conversion is the organic-bound vanadium to the residual form. However, the forms in the steam atmosphere are more diverse, by changing from the organic-bound vanadium to other forms of residue, Fe-Mn oxides and carbonates. In both atmospheres, increasing temperature promotes the decomposition of organic-bound vanadium, but the total amount in the H₂O is significantly higher than that in the CO₂ atmosphere, indicating that the CO₂ gasification atmosphere is favorable for the decomposition of organic-bound vanadium. It is worth noting that the vanadium bound to Fe-Mn oxides are gradually increasing in both atmospheres, but the amount in the steam atmosphere is three times higher than that in the CO₂ atmosphere, indicating that the steam atmosphere is conducive to the formation of Fe-Mn oxides. The presence of large amounts of Fe-Mn oxides affects the transformation of various forms in the steam gasification process. At the same time, the total amount of the residual form vanadium in the steam atmosphere is significantly lower than that of the CO₂ atmosphere, indicating that the H₂O atmosphere promotes the conversion of residual form vanadium into other forms.

As the temperature increases, the volatilization characteristic of vanadium gradually increases during H₂O and CO₂ gasification, as described in Figure 6. It is apparent that H₂O and CO₂ gasification display similar vanadium volatilization behavior. The vanadium volatility in H₂O and CO₂ gasification reaches the highest *Rv* value 1.5% and 1.8% at 1100 °C. It is obvious that the difference in the vanadium volatility between H₂O and CO₂ gasification is ignorable, so it can be concluded that the volatility of vanadium during gasification is not dependent on the gasification atmosphere, but mainly on the reaction temperature. Li et al. [18] found the volatilization of vanadium is strongly dependent on the vanadium in the organic matter in petcoke.

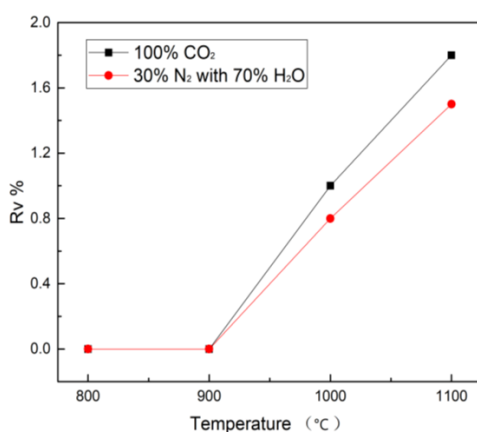


Figure 6. Volatility (*Rv*%) of vanadium during petcoke gasification from 800 °C to 1100 °C.

3.4. Ni Speciation in Different Gasification Atmospheres

As FactSage software platform is based on the Gibbs free energy minimization principle and the system is in a thermodynamic equilibrium state, it is mainly used to analyze the conversion of inorganic substances. Calculation results of CO₂ and H₂O gasification associated with Ni are shown in Figures 7 and 8.

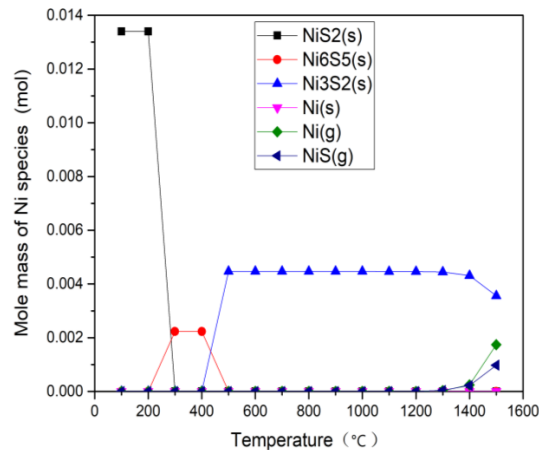


Figure 7. Calculation results of CO₂ gasification associated with Ni.

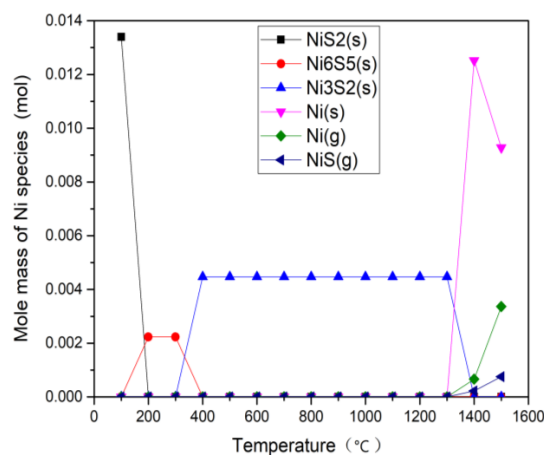


Figure 8. Calculation results of H₂O gasification associated with Ni.

For the CO₂ gasification, the only product is NiS₂ (s) below 200 °C. For the 300–400 °C temperature range, the only product changes to Ni₆S₅ (s). Above 400 °C, the main product is Ni₃S₂ (s). Li et al. [18] predicted the morphology of vanadium in the gasification of petcoke. As the temperature increased, Ni reacted with S to form NiS₂, Ni₉S₈, Ni₇S₆, and Ni₃S₂. The melting points of NiS (s) and Ni₃S₂ (s) are 645 °C and 797 °C. It can be found that the S content decreases with the increase of Ni, while the melting point and stability of Ni_xS_y compounds gradually increase. When the temperature reaches 1300 °C, gaseous Ni (g) and NiS (g) are produced. The thermodynamic equilibrium simulation in [27] showed that Ni_xS_y was the stable form of nickel until 1000 °C in a reducing gasification atmosphere (containing H₂S gas). When the temperature was up to 1000 °C, the main stable nickel form was elemental Ni. For the H₂O atmosphere, the distribution of Ni is basically the same as in the CO₂ atmosphere, but the formation temperature of Ni₆S₅ (s) and Ni₃S₂ (s) are lowered by 100 °C. This indicates that steam is favorable to generate the more stable Ni_xS_y compound, thereby suppressing the volatilization of the Ni-containing compound, which is identical with the volatility result of Ni in Figure 4. When the

temperature rises to 1400 °C, there is some solid elemental Ni apart from gaseous Ni (g) and NiS (g). Ni element does not react with other metal elements at this temperature. There are more elemental Ni (s) at high temperature in the H₂O atmosphere than that in CO₂ atmosphere, which is also consistent with the residual content of Ni at 1100 °C in the experiment (Figure 3).

When comparing the experimental data (Figure 4) with the simulation results, it is found that there is reasonable agreement on the volatilization characteristic of Ni. In the gasification process, nickel is mainly present in the form of Ni₃S₂ (with a low melting point of 797 °C). When the temperature reaches 800 °C, the volatilization of Ni species occurs, which can also be verified by the *Rv* changes in Figure 4. Wang et al. [7] investigated the corrosion and fouling in syngas cooler tubes and reported the Ni₃S₂ would be vaporized instantly during the devolatilization process due to the high temperature. It can be deduced that the main volatilization component of Ni comes from the Ni₃S₂ in the high temperature range (800–1100 °C).

3.5. V Speciation in Different Gasification Atmospheres

Figures 9 and 10 show thermodynamic calculation results of vanadium under CO₂ and H₂O gasification process. The results, under the gasification conditions of 800–1100 °C, indicate that the gaseous vanadium compounds formed in the two atmospheres are almost the same, revealing that the atmosphere has little effect on the distribution of V species at different temperatures, which proves that the volatility of V during gasification does not depend on the gasification atmosphere. Below 200 °C, the main product is V₃O₅, and it changes to V₂O₃ as the temperature rises from 300 °C to 1500 °C. Below 1300 °C, there is no volatility of V, which is consistent with the experiment results of *Rv* in Figure 6. Above 1300 °C, a little VO₂ gas is generated (less than 5% of the total amount of V). However, V₂O₃ is still the main product in the gasification process of petcoke. V does not react with other metal elements in this temperature range. The migration and conversion mechanism of V in the process of petcoke gasification is similar to that of coal gasification and the conclusions agree well with some literature [28,29] about the presence of vanadium in coal gasification reaction. Frandsen et al. [28] found that the stable V species was V₂O₃ (s) and the volatilization of VO₂ (g) emerges when the temperature exceeded 1525 °C. Bunt et al. [29] found that V₂O₃ remained stable while VO₂ gas (0.1%) was observed above 1225 °C.

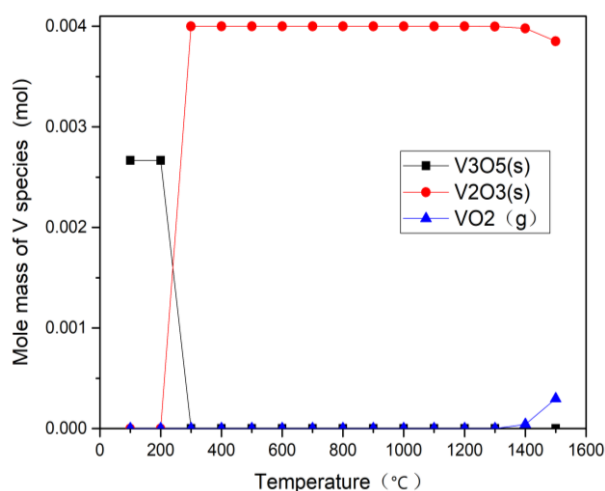


Figure 9. Calculation results of CO₂ gasification associated with V.

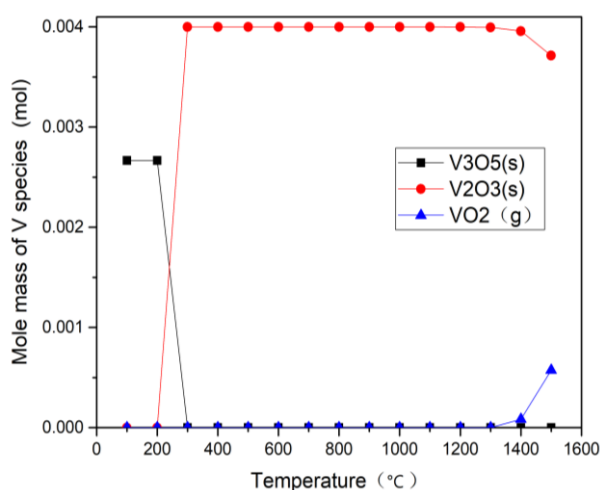
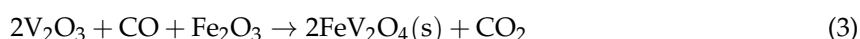


Figure 10. Calculation results of H₂O gasification associated with V.

When comparing the experimental data (Figure 4) with the simulation results, it is found that there is reasonable agreement on the volatilization characteristic of V. References [17,18,30] illustrate that the occurrence forms of V in gasification char were mainly V₂O₃, FeV₂O₄ and other forms of minerals, of which there might be the following reaction during the gasification:



Thermodynamic equilibrium calculation results show that the content of V₂O₃ (s) in H₂O and CO₂ gasification remain stable at 0.004 mol from 300 °C to 1300 °C, but it begins to decrease at 1400 °C in both H₂O and CO₂ gasification. The modeled results of the content of V₂O₃ (s) in H₂O gasification at 1400 °C and 1500 °C is 0.00396 mol and 0.00371 mol while that in CO₂ gasification is 0.00398 mol and 0.00385 mol. There is an inflection point at 1400 °C which shows the trend of the change of V compound. Therefore, the content of V₂O₃ in H₂O gasification is lower than that in CO₂ gasification at high temperature, mainly because high concentration of CO₂ inhibits the positive reaction (3), resulting the increase of residual V and decrease of Fe-Mn oxides, which is also consistent with the residual content of V at 1100 °C in the experiment (Figure 5). Combined with the occurrence patterns of vanadium, the proportion of the residual decreases and the volatile fraction increases as the temperature rises, which is also consistent with the simulation results trend. This shows that the simulation results can predict well the conversion trend of V.

3.6. Fouling, Slagging and Erosion Tendency Assessment for Ni and V Occurrence Modes

Many researchers [31–33] have found that the behavior and effects of heavy metals could not be predicted and explained by their total amount in the environment, but rather were related to the distribution of forms and the differences in migration and transformation behaviors of the various forms, which determined the volatility at high temperatures. Zhang et al. [31] concluded that the exchangeable, acid-soluble and organic matter as soluble form could be leachable under appropriate natural conditions, while insoluble forms, including the Fe-Mn oxides and residue form, were defined as the form that could not be leached. The analysis of morphological changes of heavy metals in the process of fly ash heating indicated that the soluble form of minerals decreased with increasing temperature, and the total of residual and Fe-Mn oxides form increased accordingly, summarizing that high temperature benefits the stability of minerals [31]. Liu et al. [32] found a relatively uniform distribution of five forms of Ni in dry sludge which were mainly distributed in the Fe-Mn oxides form and residue form after thermal treatment. With the increase of temperature, the ratio of state to unstable state increased from 0.4:1 in dry sludge to a maximum of 10.4:1 at 700 °C, indicating that

Ni was present in a more stable form after thermal treatment. Zorpas et al. [33] found that significant conversions of minerals converted to a less mobile form or released by vaporization during heating process. Wang et al. [7] researched the corrosion and fouling in syngas tubes, and found that the insoluble form was relatively stable and it could not be easily volatilized during the heating process, suggesting the problem of being more inclined to the erosion on the metal tube wall. Correspondingly, the soluble form was more likely to cause fouling and slagging.

Therefore, it can be seen from Figures 3 and 5 that during the gasification reaction, V and Ni dominate the erosion problem under the CO₂ atmosphere. The V and Ni insoluble mass fractions are not affected by the temperature change, remaining basically at 93% and 85%, respectively. Compared with the CO₂ atmosphere, the contribution rate of V and Ni to the fouling and slagging is obviously increased under the H₂O atmosphere, but this impact gradually weakens with the increase of temperature. The influence of atmosphere to the fouling and slagging problems is about the same at the temperature of 1100 °C. In addition, it can be noticed that the erosion problem caused by V is more serious than that by Ni under the two atmospheres, especially in the CO₂ atmosphere, so attention should be paid to the ratio of CO₂ concentration during actual operation.

4. Conclusions

The migration and transformation of V and Ni in high sulfur petcoke during CO₂ and H₂O gasification were investigated in the range from 800 °C to 1100 °C in a laboratory-scale fixed-bed reactor. The V and Ni volatilization behavior, migration and transformation behavior, and distribution of occurrence modes were studied. The main conclusions were drawn as follows:

- (1) The organic matter and residual forms were the dominant chemical forms of both V and Ni in petcoke and the Fe-Mn oxides only accounted for a small proportion.
- (2) The volatilization of V and Ni was not dependent on the gasification atmosphere, but mainly on the reaction temperature.
- (3) The CO₂ atmosphere was conducive to the conversion of the organic-bound nickel to the residual form Fe-Mn oxides. The H₂O atmosphere favors the formation of diverse forms.
- (4) Factsage results confirmed the H₂O atmosphere was favorable to suppress the volatilization of Ni-containing compounds. More residual content of V was formed in the CO₂ gasification.
- (5) The V and Ni mainly caused erosion problems under the CO₂ atmosphere while the fouling and slagging obviously increased under the H₂O atmosphere, with this impact being gradually weakened with the increase of temperature. The erosion problem caused by V was more serious than that caused by Ni, especially in the CO₂ atmosphere.

Author Contributions: W.L., B.W. and L.S. conceived, designed and performed the experiments; J.N. and W.Y. performed the sequential chemical extraction; W.L. and L.X. carried simulation calculation; W.L. and B.W. analyzed and wrote the paper.

Funding: This research was funded by the Financial support of the National Natural Science Foundation of China (NSFC) (NO. 51506068, NO. 51661145010).

Acknowledgments: This work was supported by the Financial support of the National Natural Science Foundation of China (NSFC) (NO. 51506068, NO. 51661145010). The work was also supported by the China Scholarship Council. The authors also thank the help from the Analytical and Testing Center of Huazhong University of Science and Technology.

Conflicts of Interest: The authors declare no conflict of interest.

References

1. Liu, X.; Zhou, Z.; Hu, Q.; Dai, Z.; Wang, F. Experimental Study on Co-gasification of Coal Liquefaction Residue and Petroleum Coke. *Energy Fuels* **2011**, *25*, 3377–3381. [[CrossRef](#)]
2. Zhan, X.; Jia, J.; Zhou, Z.; Wang, F. Influence of blending methods on the co-gasification reactivity of petroleum coke and lignite. *Energy Convers. Manag.* **2011**, *52*, 1810–1814. [[CrossRef](#)]

3. Hart, A.; Wood, J. In Situ Catalytic Upgrading of Heavy Crude with CAPRI: Influence of Hydrogen on Catalyst Pore Plugging and Deactivation due to Coke. *Energies* **2018**, *11*, 636. [[CrossRef](#)]
4. Glagoleva, O.F.; Strelkova, V.K.; Zhirnov, B.S.; Fatkullin, M.R.; Khairudinov, I.R. Modification of High Sulfur Petroleum Coke with Oil Shale and Its Conversion Products. *Solid Fuel Chem.* **2014**, *48*, 98–104. [[CrossRef](#)]
5. Minchener, A.J. Coal gasification for advanced power generation. *Fuel* **2005**, *84*, 2222–2235. [[CrossRef](#)]
6. Liu, X.; Wei, J.; Huo, W.; Yu, G. Gasification under CO₂-Steam Mixture: Kinetic Model Study Based on Shared Active Sites. *Energies* **2017**, *10*, 1890. [[CrossRef](#)]
7. Wang, B.; Kurian, V.; Mahapatra, N.; Martens, F.; Gupta, R. Investigation of corrosion and fouling in syngas cooler tubes. *Fuel Process. Technol.* **2016**, *141*, 202–209. [[CrossRef](#)]
8. Bryers, R.W. Utilization of petroleum coke and petroleum blends as a means of steam raising. *Fuel Process. Technol.* **1995**, *44*, 121–141. [[CrossRef](#)]
9. Jayaraman, K.; Gokalp, I. Gasification characteristics of petcoke and coal blended petcoke using thermogravimetry and mass spectrometry analysis. *Appl. Therm. Eng.* **2015**, *80*, 10–19. [[CrossRef](#)]
10. Park, W.; Oh, M.S. Slagging of petroleum coke ash using Korean anthracites. *J. Ind. Eng. Chem.* **2008**, *14*, 350–356. [[CrossRef](#)]
11. Nakano, J.; Sridhar, S.; Moss, T.; Bennett, J.; Kwong, K. Crystallization of Synthetic Coal–Petcoke Slag Mixtures Simulating Those Encountered in Entrained Bed Slagging Gasifiers. *Energy Fuels* **2009**, *23*, 4723–4733. [[CrossRef](#)]
12. Duchesne, M.A.; Ilyushechkin, A.Y.; Hughes, R.W.; Lu, D.Y.; McCalden, D.J.; Macchi, A.; Anthony, E.J. Flow behaviour of slags from coal and petroleum coke blends. *Fuel* **2012**, *97*, 321–328. [[CrossRef](#)]
13. Mahapatra, N.; Kurian, V.; Wang, B.; Martens, F.; Gupta, R. Pyrolysis of asphaltenes in an atmospheric entrained flow reactor: A study on char characterization. *Fuel* **2015**, *152*, 29–37. [[CrossRef](#)]
14. Brüggemann, P.; Baitalow, F.; Seifert, P.; Meyer, B.; Schlichting, H. Behaviour of heavy metals in the partial oxidation of heavy fuel oil. *Fuel Process. Technol.* **2010**, *91*, 211–217. [[CrossRef](#)]
15. Querol, X.; Alastuey, A.; Lopez-Soler, A.; Plana, F.; Fernandez-Turiel, J.L.; Zeng, R.; Xu, W.; Zhuang, X.; BSpino, B. Geological controls on the mineral matter and trace elements of coals from the Fuxin basin, Liaoning Province, northeast China. *Int. J. Coal Geol.* **1997**, *34*, 89–109. [[CrossRef](#)]
16. Dai, S.; Ren, D.; Tang, Y.; Yue, M.; Hao, L. Concentration and distribution of elements in Late Permian coals from western Guizhou Province, China. *Int. J. Coal Geol.* **2005**, *61*, 119–137. [[CrossRef](#)]
17. Wang, Z.; Bai, J.; Kong, L.; Bai, Z.; Li, W. Effect of V and Ni on Ash Fusion Temperatures. *Energy Fuels* **2013**, *27*, 7303–7313. [[CrossRef](#)]
18. Li, J.; Zhao, J.; Zhang, L.; Liu, T.; Fang, Y. Transformation behavior of vanadium in petroleum coke during high temperature CO₂-gasification. *Fuel* **2017**, *194*, 83–90. [[CrossRef](#)]
19. Lu, H.; Chen, H.; Li, W.; Li, B. Occurrence and volatilization behavior of Pb, Cd, Cr in Yima coal during fluidized-bed pyrolysis. *Fuel* **2004**, *83*, 39–45. [[CrossRef](#)]
20. Liu, S.; Qiao, Y.; Lu, Z.; Gui, B.; Wei, M.; Yu, Y.; Xu, M. Release and Transformation of Sodium in Kitchen Waste during Torrefaction. *Energy Fuels* **2014**, *28*, 1911–1917. [[CrossRef](#)]
21. Kolker, A.; Huggins, F.E.; Palmer, C.A.; Shah, N.; Crowley, S.S.; Huffman, G.P.; Finkelman, R.B. Mode of occurrence of arsenic in four US coals. *Fuel Process. Technol.* **2000**, *63*, 167–178. [[CrossRef](#)]
22. Liu, Y.; Ma, L.; Li, Y.; Zheng, L. Evolution of heavy metal speciation during the aerobic composting process of sewage sludge. *Chemosphere* **2007**, *67*, 1025–1032. [[CrossRef](#)] [[PubMed](#)]
23. Tessier, A.; Campbell, P.G.C.; Bisson, M. Sequential Extraction Procedure for the Speciation of Particulate Trace Metals. *Anal. Chem.* **1979**, *51*, 844. [[CrossRef](#)]
24. Li, J.; Wang, X.; Wang, B.; Zhao, J.; Fang, Y. Investigation on the fates of vanadium and nickel during co-gasification of petroleum coke with biomass. *Bioresour. Technol.* **2018**, *257*, 47–53. [[CrossRef](#)] [[PubMed](#)]
25. Bale, C.W.; Chartrand, P.; Degterov, S.A.; Eriksson, G.; Hack, K.; Ben Mahfoud, R.; Melançon, J.; Pelton, A.D.; Petersen, S. FactSage Thermochemical Software and Databases. *Calphad* **2002**, *26*, 189–228. [[CrossRef](#)]
26. Li, J.; Zhao, J.; Guo, S.; Zhou, X.; Liu, Y.; Bai, J.; Fang, Y. Predicting the vanadium speciation during petroleum coke gasification by thermodynamic equilibrium calculation. *Fuel* **2016**, *176*, 48–55. [[CrossRef](#)]
27. Liu, S.; Wang, Y.; Yu, L.; Oakey, J. Thermodynamic equilibrium study of trace element transformation during underground coal gasification. *Fuel Process. Technol.* **2006**, *87*, 209–215. [[CrossRef](#)]
28. Frandsen, F.; Dam-Johansen, K.; Rasmussen, P. Trace elements from combustion and gasification of coal—An equilibrium approach. *Prog. Energy Combust. Sci.* **1994**, *20*, 115–138. [[CrossRef](#)]

29. Bunt, J.R.; Waanders, F.B. Trace element behaviour in the Sasol-Lurgi fixed-bed dry-bottom gasifier. Part 3—The non-volatile elements: Ba, Co, Cr, Mn, and V. *Fuel* **2010**, *89*, 537–548. [[CrossRef](#)]
30. Li, J.; Zhao, J.; Dai, X.; Bai, J.; Fang, Y. Effect of Vanadium on the Petroleum Coke Ash Fusibility. *Energy Fuels* **2017**, *31*, 2530–2537. [[CrossRef](#)]
31. Zhang, H.; Zhao, Y.; Qi, J. Thermal property of heavymetals in MSWI fly ash. *Environ. Pollut. Control* **2007**, *29*, 9–13.
32. Liu, S.; Li, A.; Yuan, W. Effect of temperature on the heavy metal fraction distribution and comprehensive toxicity on incineration residue of sewage sludge. *J. Saf. Environ.* **2008**, *1*, 43–47.
33. Zorpas, A.A.; Vlyssides, A.G.; Zorpas, G.A.; Karlis, P.K.; Arapoglou, D. Impact of thermal treatment on metal in sewage sludge from the Psittalias wastewater treatment plant, Athens, Greece. *J. Hazard. Mater.* **2001**, *82*, 291–298. [[CrossRef](#)]



© 2018 by the authors. Licensee MDPI, Basel, Switzerland. This article is an open access article distributed under the terms and conditions of the Creative Commons Attribution (CC BY) license (<http://creativecommons.org/licenses/by/4.0/>).